

## Article

# Energy Absorption of Square Tubes Filled by Modularized Honeycombs with Multiple Gradients

Zhen Li <sup>\*</sup>, Zhengyang Kang and Xiaoping Su

School of Mechanical and Power Engineering, Nanjing Tech University, Nanjing 211800, China

\* Correspondence: zhenli@njtech.edu.cn

**Abstract:** The Uniform Honeycomb-filled Tube (UHT) is one of the composite structures that has shown huge potential in absorbing energy. In this paper, Uniform Honeycomb (UH) filler is replaced by an enhanced Modularized Honeycomb (MH). The biggest advantage of MH is that it can significantly enhance energy absorption without adding weight compared with its uniform counterpart. Finite element models are created, and then validated by theoretical models. The energy absorption of the Modularized Honeycomb-filled Tube (MHT) is compared with that of the empty tube and UHT. The results show that the MHT is superior to them in Specific Energy Absorption (SEA). It is also found that the tube can help the MH improve its deformation stability, which is the key of the MHT's excellent energy absorption capacity. Then, effects of design parameters on the SEA of the MHT are investigated and discussed. The results show that the MH with a large graded coefficient is good for enhancing the SEA of the MHT. However, the SEA also relies on the match between the honeycomb filler and tube walls. The work could inspire designs of modularized filler with various types of cells and benefit the development of advanced energy absorbers with lighter weight and more excellent energy absorption capacity.

**Keywords:** square tube; modularized honeycomb filler; quasi-static compression; deformation mode; energy absorption

**Citation:** Li, Z.; Kang, Z.; Su, X.Energy Absorption of Square Tubes Filled by Modularized Honeycombs with Multiple Gradients. *Machines* **2023**, *11*, 294. <https://doi.org/10.3390/machines11020294>Academic Editor:  
Dimitrios Manolakos

Received: 13 January 2023

Revised: 6 February 2023

Accepted: 14 February 2023

Published: 15 February 2023



**Copyright:** © 2023 by the authors. Licensee MDPI, Basel, Switzerland. This article is an open access article distributed under the terms and conditions of the Creative Commons Attribution (CC BY) license (<https://creativecommons.org/licenses/by/4.0/>).

## 1. Introduction

Tubular structures and honeycombs are both well-known energy absorption devices. On one hand, when they are subjected to compression, their high porosities allow them to deform from large volume to densified state, thus experiencing a large displacement of energy absorption. On the other hand, the plateau characteristic allows them to absorb energy in a stable manner [1–6]. Therefore, they have attracted much attention in crash protection for the last few decades. However, with the rapid development of the modern automotive, aerospace and military industries, more powerful energy absorption devices are needed. Aiming to develop excellent energy absorbers and reduce costs, researchers filled honeycombs into tubes to make composite Honeycomb-filled Tubes (HT). Their combination could give rise to more excellent energy absorption capacity per unit mass [7], and thus, this kind of composite structure is worthy of deep investigation.

In addition to honeycomb, foam cannot be avoided when talking about filling materials. The reasons for choosing honeycomb as the filler in this paper are two-fold. First, honeycomb consists of periodic cells that are easier to design compared with foam. Second, honeycomb is more weight efficient than foam, leading to the superiority of honeycomb-filled tubes in specific energy absorption [8]. In terms of improving the energy absorption capacity of honeycombs, research is first conducted on investigating the effects of the geometric parameters of many different honeycombs on strength and energy absorption capacity. Taking hexagonal honeycomb as an example, increasing cell-wall thickness is able to improve both its in-plane and out-of-plane strengths and energy absorption abilities [9]. Cell-wall angle and cell-wall length are also key parameters for property enhancement [10–12]. For instance,

Hu et al. [11,12] pointed out that a cell-wall angle of  $45^\circ$  is the optimal design for excellent energy absorption capacity and low crushing velocity sensitivity under  $y$ -directional compression. When cell-wall thickness and cell-wall length are both varied, the strength of honeycomb may stay the same as long as the ratio of these two parameters is constant, which can be used to reduce costs in numerical simulation [13]. However, varying geometric parameters will also lead to the change of the honeycomb's weight, and thus, it may not be weight efficient, i.e., the energy absorption per unit mass may not be improved with the enhancement of strength. Functional graded design, by contrast, is able to enhance the energy absorption of honeycomb without adding weight to the structure. Traditionally, graded honeycomb is designed via gradually varying the mechanical properties of honeycomb along a certain direction. The main approach of realizing the gradient is to vary the cell geometry (such as cell-wall length, cell-wall angle and cell-wall thickness) and base material [10,14–18]. It has been proved that when applying graded design along the loading direction, the honeycomb shows a stair-like stress curve, a more controllable collapse mode and enhanced energy absorption capacity compared with that of its uniform counterpart [17,18]. When applying a gradient along the perpendicular direction of the loading, the honeycomb shows an enhanced plateau stress feature that gives rise to more excellent energy absorption capacity [19–21]. There are also several studies proposing multi-directional graded honeycombs. For example, Wu et al. [22] proposed a honeycomb structure with both in-plane and out-of-plane gradients; results show that it can improve energy absorption capacity and reduce initial peak force. Recently, the authors proposed a MH that possesses gradients in two mutually orthogonal directions that are perpendicular to the loading. They proved that, compared with uniform honeycomb, modularized honeycomb is able to double energy absorption capacity [23].

On the topic of honeycomb-filled tubes, research was first conducted on the energy absorption of UHT. It was found that filling honeycombs into the tube was better than simply thickening empty tube walls [8]. Moreover, the energy absorption of UHT outperforms that of the sum of its two components compressed individually, which stems from the fact that the interaction between tube and honeycomb also makes a contribution to energy absorption [24]. In addition, when tube walls dominate the deformation process, this helps honeycomb fillers improve deformation stability, which is the key to energy absorption [13,25]. In comparison with foam-filled tubes, honeycomb-filled tubes are more promising and efficient in developing lightweight energy absorbers [8]. Given the above-mentioned advantages, much research was conducted to develop efficient honeycomb-filled tubes. Part of research focus is on the effects of different cross-sections of tubes and different types of honeycomb fillers on developing powerful energy absorption structures [7,26–36]. Meanwhile, lightweight is one of the keywords throughout the whole research process. For example, instead of fully filling multi-cell tubes with honeycombs, local filling can be more efficient in achieving both excellent energy absorption and light weight [35,36]. Another part focuses on applying functionally graded design to filled structures. In general, gradient is applied to honeycomb filler or tube along the loading direction. This kind of design has controllable deformation modes, and it is able to reduce initial peak force and enhance energy absorption capacity compared with those of uniform honeycomb-filled structures [37–42]. There are also some studies that employed gradient to both filler and tube, also known as multiple graded filled structures. Compared with traditional graded filled structures, this design could have even more excellent energy absorption capacity [43–45]. Moreover, multiple gradients will give rise to more flexibilities in designing energy absorbers with controllable deformation, initial peak force and energy absorption capacity. In addition to the above approaches, replacing the traditional materials of filled structures with advanced materials such as Carbon Fiber Reinforced Polymer (CFRP) is also a popular approach to acquire excellent energy absorption with light weight [46,47].

The above literature review and our research experience remind us that the combination of tube and modularized honeycomb may be able to develop excellent energy absorption structures. However, to the best of the authors' knowledge, the energy absorption of MHTs has not been studied, and the effects of the design parameters of the tube

and filler on energy absorption have yet to be investigated. Understanding the energy absorption capacity of MHTs could benefit the design and development of energy absorption devices with light weight and excellent energy absorption.

In this paper, modularized honeycomb is filled into the square tube to develop novel energy absorbers. The assessment of the energy absorption capacity of MHTs is conducted by analyzing quasi-static compression results obtained from finite element simulations. The rest of this paper is arranged as follows. Section 2 describes the geometry of the proposed modularized honeycomb-filled square tube and creates finite element models for the following analyses. Model validation is also conducted in this section by introducing well-known theoretical models. Section 3 compares the energy absorption capacity of MHTs with that of UHTs and empty tubes and investigates the effects of design parameters on the energy absorption capacity of MHTs. Concluding remarks are presented in Section 4.

## 2. Square Tube Filled with Modularized Honeycomb

### 2.1. Model Description

Modularized design is a graded design that arranges honeycomb modules with a different relative density in two mutually orthogonal directions. For example, Figure 1a shows regular hexagonal modularized honeycomb with  $3 \times 3$  modules arranged in  $x$  and  $y$  directions. All modules consist of cells with the same shape geometry, i.e., all modules have the same cell-wall length  $l$ . However, each module possesses unique cell-wall thickness ( $T_{11} \sim T_{33}$ ); in each case, each of them has unique relative density and mechanical properties. All the modules are set to have the same  $x$ - $y$  cross-section; the average relative density of modularized honeycomb can then be obtained by averaging the summary of relative densities of all the modules

$$\bar{\rho} = \frac{\sum_{i=1}^n \sum_{j=1}^m \bar{\rho}_{ij}}{nm} \quad (1)$$

where  $\bar{\rho}_{ij}$  is the relative density of the  $ij$ th module;  $n$  and  $m$  are the number of modules in  $x$  and  $y$  directions, respectively. For regular hexagonal honeycomb, relative density of each module can be calculated by [9]

$$\bar{\rho}_{ij} = \frac{2}{\sqrt{3}} \frac{T_{ij}}{l} \quad (2)$$

where  $l$  is cell-wall length. In the authors' previous study, the relation of relative density between modules is defined as [23]

$$\lambda_x = \left| \frac{\bar{\rho}_{1j} - \bar{\rho}_{2j}}{\bar{\rho}_{(1:n)j}} \right| \quad (3)$$

$$\lambda_y = \left| \frac{\bar{\rho}_{i1} - \bar{\rho}_{i2}}{\bar{\rho}_{i(1:m)}} \right| \quad (4)$$

where  $\bar{\rho}_{(1:n)j}$  and  $\bar{\rho}_{i(1:m)}$  indicate average relative densities of modules in the  $j$ th and  $i$ th columns, respectively. It has been proved that the strength and energy absorption of a  $5 \times 5$  MH made of regular hexagonal honeycomb can achieve more than twice its uniform counterpart in  $x$  direction when assigning relative density gradients of modules in the way of Figure 1b [23]. More importantly, the proposed modularized honeycomb and its uniform counterpart (i.e., uniform honeycomb) have the same overall size, relative density and weight. Therefore, this design is perfect for engineering applications with requirements of light weight, high strength and excellent energy absorption capacity.

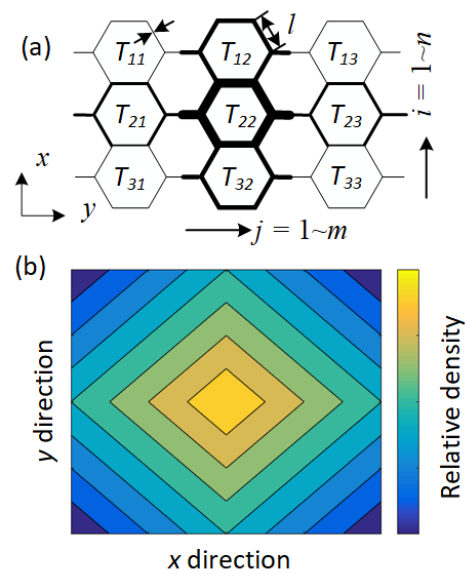


**Figure 1.** Diagram and density distribution of modularized honeycomb (a) definition of cell-wall thicknesses (b) relative density distribution of modules.  $x$  and  $y$  axes indicate the directions of gradients. The relative density of modules increases from dark blue color to bright yellow color.

As discussed in Section 1, the combination of honeycomb and tube has huge potentials in absorbing energies. Filling MH into the tube may further enhance honeycomb-filled structures. To this end, this paper intends to fill a tube with MH. Specifically, a MH is filled into a square tube, see Figure 2. The size of the square tube is  $W = 50$  mm,  $H = 100$  mm; the inner honeycomb is designed to be a  $5 \times 5$  modularized honeycomb made of regular hexagonal cells with cell-wall length of  $l = 3.33$  mm. All the modules have the same area of  $x$ - $y$  cross-section. The reason a  $5 \times 5$  configuration is selected is that it can show both the advantages and drawbacks of MH filler in absorbing energy and how the tube helps the honeycomb filler improve its deformation stability when they work together. Details are shown in the following analyses. The  $x$ - $y$  cross-section of the modularized honeycomb is designed to be a square shape to fit the square tube, see the MH filler in Figure 2.

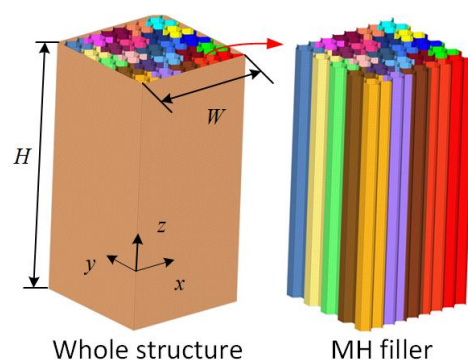


**Figure 2.** Diagram of square tube filled with modularized honeycomb. Different colors indicate different modules in the modularized honeycomb filler.

## 2.2. Finite Element Model

To investigate the energy absorption capacity of the modularized honeycomb-filled tube, a Finite Element (FE) model is created by using Hypermesh (Altair Engineering, Inc., Troy, MI, United States). Four-node shell elements are created on the middle faces of thin walls of both the tube and honeycomb filler. Finite Element analysis is conducted by means of the Abaqus/Explicit solver. Two rigid plates are placed on the top and bottom of the modularized honeycomb-filled tube along the  $z$  direction. During simulation, the top one

is given a constant velocity of 1 m/s to simulate quasi-static compression [23]. The bottom one is fixed to support the structure. The compression displacement of the top plate is set to 75% of the structure's height. Hard contact and penalty friction contact are applied to normal and tangential interactive behaviors, respectively. In Abaqus, 'General Contact' is applied to configure above interactions; the friction coefficient is 0.2 [29,36]. Unless stated otherwise, the average relative density of the honeycomb is 0.04 and the wall thickness of the square tube is 1.5 mm. For the purposes of symmetry, we let  $\lambda_x = \lambda_y = \lambda_z$  in the following investigations. Mesh convergence analysis is conducted; the size of 1 mm for both tube and honeycomb filler is considered to be perfect for guaranteeing both simulation accuracy and efficiency.

### 2.3. Material Properties

The base materials of tube and honeycomb filler are steel and AlSi10Mg, respectively. The mechanical properties of steel are density  $\rho_s = 7800 \text{ kg/m}^3$ , elastic modulus  $E = 210 \text{ GPa}$ , Poisson's ratio  $\mu = 0.3$ , yield strength  $\sigma_y = 200 \text{ MPa}$  and ultimate stress  $\sigma_u = 400 \text{ MPa}$ . The engineering strain versus stress curve under the standard tensile test are shown in Figure 3a [48]. The mechanical properties of AlSi10Mg are density  $\rho_s = 2530 \text{ kg/m}^3$ , elastic modulus  $E = 70 \text{ GPa}$ , Poisson's ratio  $\mu = 0.3$ , yield strength  $\sigma_y = 228 \text{ MPa}$  and ultimate stress  $\sigma_u = 326 \text{ MPa}$ . The engineering strain versus stress curve under the standard tensile test are shown in Figure 3b [29]. All the tensile experiments are performed under the ASTM E8 Standard Test with quasi-static loadings.

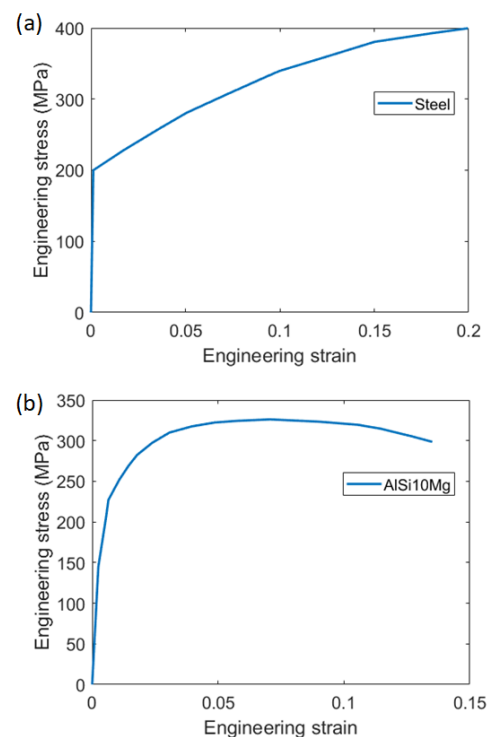


**Figure 3.** Engineering strain—stress curves of materials (a) Steel (b) AlSi10Mg.

### 2.4. Model Validation

Hanssen et al. [49] developed the theoretical expression for predicting the quasi-static mean crushing force of the empty square tube

$$F_{tube} = 13.06\sigma_0 b^{1/3} T_t^{5/3} \quad (5)$$

where  $b$  is the edge length of the square cross-section;  $T_t$  is the wall thickness of the tube.  $\sigma_0$  is the flow stress of the base material calculated by

$$\sigma_0 = \sqrt{\frac{\sigma_y \sigma_u}{1 + n'}} \quad (6)$$

where  $n'$  is the strain hardening exponent. The theoretical model for predicting the quasi-static mean crushing force of the uniform hexagonal honeycomb in the out-of-plane direction is expressed as [50]

$$F_{\text{honeycomb}} = 6.63\sigma_0(T/l)^{5/3}A \quad (7)$$

where  $T$  and  $l$  are cell-wall thickness and length, respectively.  $A$  is the area of the cross-section of the honeycomb.

Then, the above theoretical models are used to validate FE models presented in Section 2.2. Comparisons between theoretical and FE models are shown in Figure 4. As can be seen, both results are in good agreement in the plateau area, which validates the effectiveness and accuracy of the FE models created in this paper.

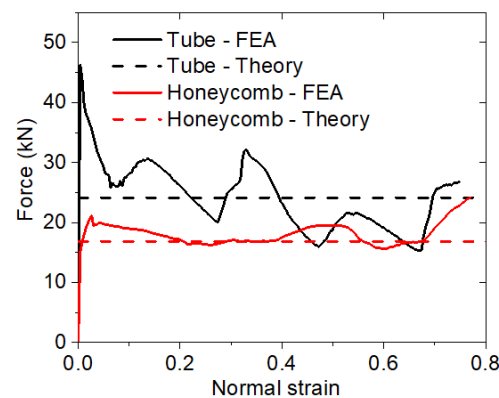


Figure 4. Comparison between finite element and theoretical results.  $T_t$  is 1.5 mm,  $\bar{\rho} = 0.04$ .

### 3. Energy Absorption of Modularized Honeycomb-Filled Square Tube

#### 3.1. Deformation Stability of Honeycomb Filler

Figure 5 shows the results of the MH ( $\lambda_2 = 0.8$ ) and its corresponding UH (i.e., uniform honeycomb with the same relative density as MH) under  $z$  direction compression. Through compressing honeycombs individually, it is found that UH mainly deforms in the vertical direction (compression direction) under quasi-static compression, see Figure 5a. However, for MH with large value of graded coefficient, instead of deforming vertically, may exhibit a buckling deformation mode; see the example shown in Figure 5b, indicating that deformation of MH is not as stable as that of UH. This stems from the fact that different relative densities of modules in MH lead to different mechanical properties, causing different reactions under quasi-static compression. As a result, the uneven deformation of modules in MH makes it easier to lose its stability than that of UH during quasi-static compression. The reaction force and energy absorption are, consequently, influenced by the deformation mode, see Figure 5c,d. When MH starts to buckle, the reaction force decreases dramatically to a relatively low level, indicating that MH loses most of its ability to resist the compression, see Figure 5c. In the aspect of energy absorption, specific energy absorption is used to evaluate energy absorption per unit mass of these structures, which can be calculated by

$$E_s = \frac{E_i}{M} \quad (8)$$

where  $E_i$  is the energy absorbed by the structure during compression;  $M$  is the weight of the structure.

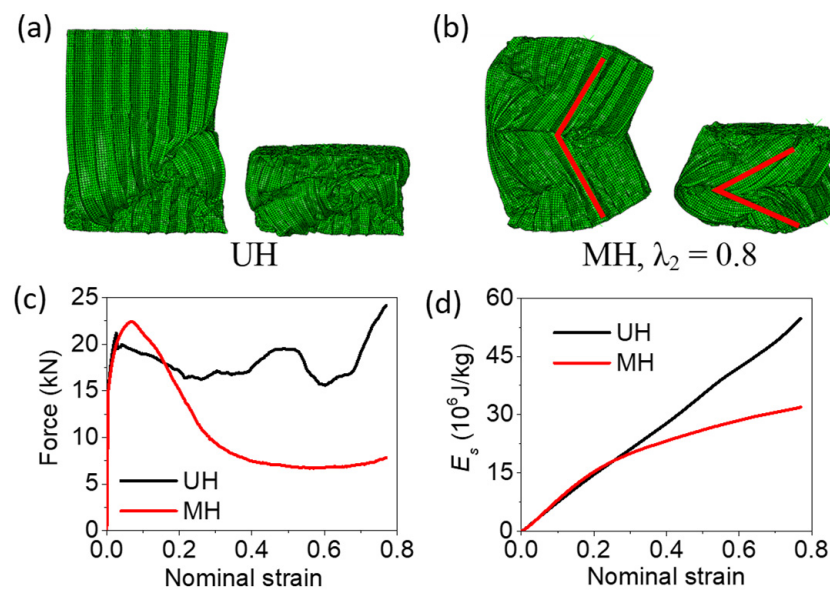


**Figure 5.** Comparisons between UH and MH with  $\bar{\rho} = 0.08$  under quasi-static compression. (a) deformation mode of UH, (b) deformation mode of MH, (c) reaction force, (d) specific energy absorption.

As can be seen in Figure 5d, the SEA of MH decreases by 41.77% at a nominal strain of 0.75 compared with that of UH. Such weakening in SEA indicates that the buckling deformation mode is not good for energy absorption and should be avoided.

To investigate the deformation stability of honeycomb filler in tubes, MHs with different graded coefficients are filled into tubes with different thicknesses from 1 mm to 3 mm. Table 1 shows the results of deformation of honeycomb fillers in tubes; ‘√’ indicates that honeycomb filler experiences mainly vertical deformation during compression while ‘×’ indicates that honeycomb filler buckles during compression. As can be seen, when the wall thickness of the tube is thin ( $T_t = 1$  mm, 1.5 mm, 2 mm), it experiences deformation mode 1, see Figure 6a. In this case, the interaction between the tube and honeycomb filler is able to guarantee the deformation stability of the honeycomb filler in most cases. Exceptions occur when three conditions are met: (1) the average relative density of the honeycomb filler is large, (2) the graded coefficient of the honeycomb filler is large ( $\lambda_2 = 0.8$ ), (3) the tube is very thin ( $T_t = 1$  mm, 1.5 mm), see Table 1. This indicates that when both the average relative density and graded coefficient of the honeycomb filler are large, the buckling deformation of the honeycomb filler is too strong to be limited by the tube with thin wall thickness. In other words, tube walls must be strong enough to limit the buckling of the honeycomb filler, so that the honeycomb filler can deform in a stable manner. When the wall thickness of the tube is thick ( $T_t = 2.5$  mm, 3 mm), it experiences deformation mode 2, see Figure 6b. In this case, the space in the tube is larger than that of tubes with thin thickness during deformation, which gives the honeycomb filler more space to deform laterally. This weakens the interaction between tube walls and honeycomb filler. In this case, the tube can barely help the honeycomb filler improve deformation stability when the honeycomb filler tends to buckle. As a result, the deformation instability of the MH filler in thick tubes occurs earlier ( $\lambda_2 = 0.6$ ) than in those filled in thin tubes, see Table 1. Overall, the deformation stability of the honeycomb filler can be improved by filling it into tubes; such improvement would benefit the energy absorption of the filled structure.

**Table 1.** Deformation stability of honeycomb fillers when different thicknesses of tubes are applied.

$\bar{\rho}$	$\lambda_2$	$T_t$ (mm)				
		1	1.5	2	2.5	3
0.04	0	✓	✓	✓	✓	✓
	0.4	✓	✓	✓	✓	✓
	0.6	✓	✓	✓	×	×
	0.8	✓	✓	✓	×	×
0.06	0	✓	✓	✓	✓	✓
	0.4	✓	✓	✓	✓	✓
	0.6	✓	✓	✓	×	×
	0.8	✓	✓	✓	×	×
0.08	0	✓	✓	✓	✓	✓
	0.4	✓	✓	✓	✓	✓
	0.6	✓	✓	✓	×	×
	0.8	×	✓	✓	×	×
0.1	0	✓	✓	✓	✓	✓
	0.4	✓	✓	✓	✓	✓
	0.6	✓	✓	✓	✓	×
	0.8	×	✓	✓	×	×
0.12	0	✓	✓	✓	✓	✓
	0.4	✓	✓	✓	✓	✓
	0.6	✓	✓	✓	✓	✓
	0.8	×	×	✓	×	×

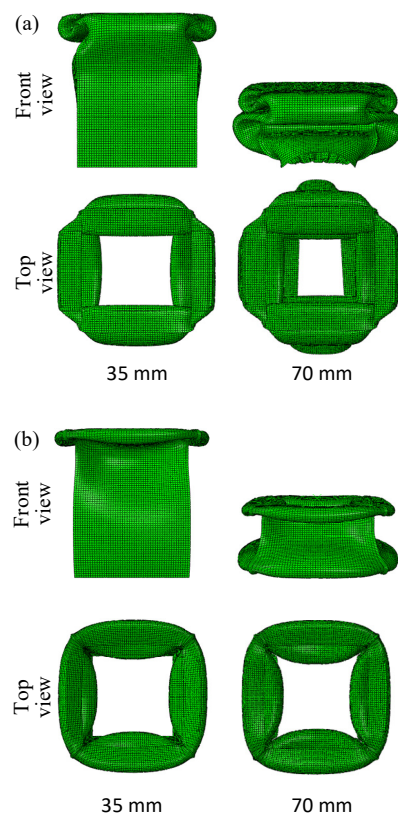


**Figure 6.** Deformation modes of tubes. (a) deformation mode 1 of tube with  $T_t = 1.5$  mm, (b) deformation mode 2 of tube with  $T_t = 3$  mm.



### 3.2. Effects of Honeycomb Design Parameters

Though it has been proved that MH is able to absorb more energy than that of UH [23], it is not clear that whether MH can enhance MHTs given that the deformation of the filled structure is more complicated than that of the individual honeycomb or tube. To examine energy absorption capacity, quasi-static compressions are conducted. For comparison purposes, empty tubes and UHTs are also compressed. All tube walls are given a thickness of 1.5 mm, and the average relative density of all honeycomb fillers is 0.04. For MH filler, it is given a graded coefficient  $\lambda_2 = 0.8$ . Figure 7 shows results of force and specific energy absorption with respect to nominal strain, respectively. It can be seen that in the plateau area, the empty tube exhibits the lowest level of force among them, see the black dash curve in Figure 7a. When a UH is filled into the tube, the force increases to a higher level, indicating that the uniform honeycomb filler makes a positive contribution to the strength of the whole structure. When UH is replaced by a MH with  $\lambda_2 = 0.8$ , the force level is further enhanced, resulting in the highest strength among these three cases, see the red solid curve in Figure 7a. This indicates that with the same weight, MH could help improve the strength of MHTs compared with that of UH.

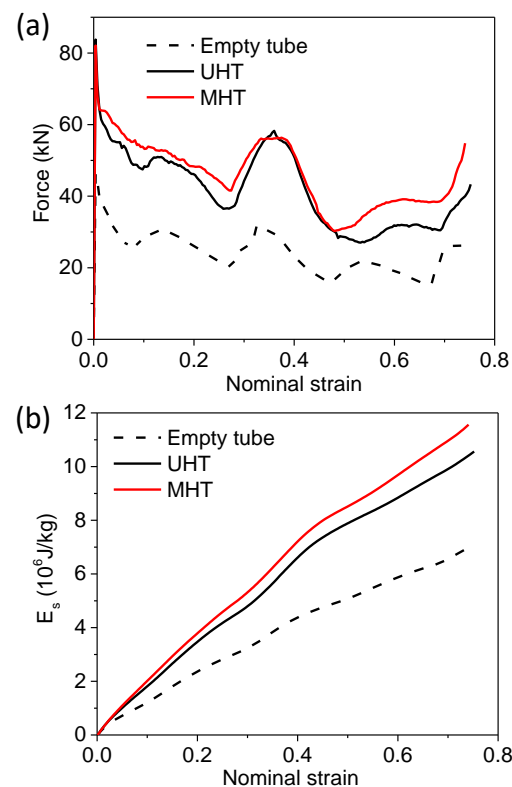


**Figure 7.** Comparisons of quasi-static results between empty and filled tubes,  $T_t$  is 1.5 mm,  $\bar{\rho} = 0.04$  and  $\lambda_2$  is 0 and 0.8 for UH and MH, respectively. (a) reaction force, (b) specific energy absorption.

As can be seen in Figure 7b, the empty tube absorbs the least energy per unit mass at the end of the compression process. When UH is filled into the tube, the specific energy absorption of the whole structure is significantly enhanced, which is 49.5% larger than that of the empty tube at a nominal strain of 0.75. The strongest energy absorption capacity is shown when MH with  $\lambda_2 = 0.8$  is filled into the tube, see the red solid curve in Figure 7b. Compared with those of the empty tube and UHT, the specific energy absorbed by the MHT is enhanced by 63.85% and 9.47% at a nominal strain of 0.75, respectively. This indicates that the MHT can absorb more energy than the UHT. Moreover, since the MHT has the same weight as the UHT, it could benefit the development of lightweight energy absorbers.

To investigate how MH enhances the strength and energy absorption of the filled structure, the contributions of the tube and honeycomb filler to the energy absorption of

the whole structure are investigated. Deformation modes and the energy absorption of these two components are captured from the above numerical simulations and shown in Figures 8 and 9, respectively. As can be seen, not only empty tubes but also filled tubes are all in deformation mode 1 during compression. However, the lateral deformation (inner folding deformation) of tube walls is varied as different honeycomb is filled, see Figure 8. This is due to the fact that the resisting strength (lateral strength) of the honeycomb filler limits the inner folding deformation of the tube walls during compression. This interaction between honeycomb and tube walls is critical since it could give rise to the enhancement of the energy absorption of the filled structures [13]. When UH is replaced by MH, lateral deformation increases a little bit, see Figure 8, indicating that MH is not as strong as UH in resisting the lateral deformation of tube walls. This can be easily explained by the fact that, according to the gradient design of Figure 1, the outer modules of MH have relatively low relative density, resulting in weak resistance to tube walls during inner folding. In terms of energy absorption, this weak resistance leads to a 5.11% decrease in the energy absorption of the tube at a nominal strain of 0.75, see the black solid and dash curves in Figure 9. Nevertheless, MH filler with  $\lambda_2 = 0.8$  absorbs 32.09% more energy than UH filler at a nominal strain of 0.75, see the red solid and dash curves in Figure 9. As a result, the MHT absorbs 9.47% more energy than the UHT with the same weight. This indicates that, compared with filling UH, filling MH into the tube has potential in further enhancing the strength and energy absorption of the honeycomb-filled tube as long as the enhancement of the energy absorption of MH is able to exceed the loss of energy absorption caused by the weakening of the interaction between tube walls and honeycomb filler.

The above example has shown that filling MH in square tubes could be a better choice than that of filling UH to enhance the strength and energy absorption of the filled structure. The next question is how to design MH and tube walls to obtain excellent energy absorption capacity. Therefore, the effects of average relative density and the graded coefficients of honeycomb are investigated and discussed.

In this research, graded coefficient  $\lambda_2$  and average relative density  $\bar{\rho}$  are varied in ranges of 0~0.8 and 0.04~0.12, respectively. Tube wall thickness is set to 1.5 mm. Figure 10 shows the specific energy absorption of the filled structure as well as the contributions of its two components to energy absorption at a nominal strain of 0.75. Given that the strength of the outer modules of MH weakens as graded coefficient  $\lambda_2$  increases, interaction that resists inner folding of tube walls also weakens. As a result, the contribution of the tube to the specific energy absorption of the filled structure slightly decreases as graded coefficient  $\lambda_2$  increases. However, the energy absorption of MH is enhanced remarkably with the increase in graded coefficient  $\lambda_2$ . Overall, when a MH with  $\bar{\rho} = 0.04$  is filled into the tube, the specific energy absorption of the filled structure exhibits an increasing trend with the increase in graded coefficient  $\lambda_2$ , see Figure 10a. When  $\bar{\rho}$  equals to 0.06 or 0.08, similar trends are observed, see Figure 10b,c. The above observations indicate that the energy absorption enhancement of MH is able to exceed the loss of energy absorption caused by the weakness of interaction, and thus, the MHT can absorb more energy per unit mass than that of the UHT when MH with  $\bar{\rho} = 0.04 \sim 0.08$  is filled into the tube.

When a honeycomb with  $\bar{\rho} = 0.1$  is applied, the specific energy absorption of the MHT does not always outperform that of the UHT. Unlike that discussed in the prior paragraph, the MHT absorbs the least energy when  $\lambda_2 = 0.4$ , see Figure 10d. To find out the reason behind this, deformation modes are shown in Figure 11a. It is clear to observe that when a UH is filled into the tube, four lobes are generated on the tube at the end of the compression. This is caused by the fact that the lateral strength of the UH is strong enough to force tube walls to fold in a shorter length and generate more lobes. As a result, more energy is absorbed by these lobes when UH is applied. By contrast, the weak lateral strength of MH with  $\lambda_2 = 0.4$  does not have the ability to force the tube walls to make more lobes, see Figure 11a. The reduction in the number of lobes leads to less energy absorbed by the tube. Meanwhile, the enhancement of MH with  $\lambda_2 = 0.4$  is not able to make up for the loss caused by the reduction of lobes. As a result, the MHT with  $\lambda_2 = 0.4$  absorbs less energy than that of

the UHT. When MH with  $\lambda_2 = 0.8$  is filled into the tube, the enhancement of the MH filler exceeds the loss caused by the reduction of lobes, and thus, MHTs absorb the most energy per unit mass among these three cases, see Figure 10d.

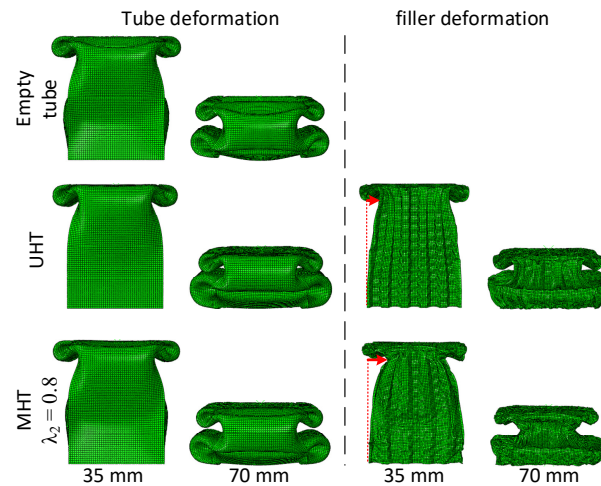


**Figure 8.** Comparisons of deformation modes of empty tube, UHT and MHT.  $T_t$  is 1.5 mm,  $\bar{\rho} = 0.04$ ,  $\lambda_2$  is 0 and 0.8 for UH and MH, respectively.

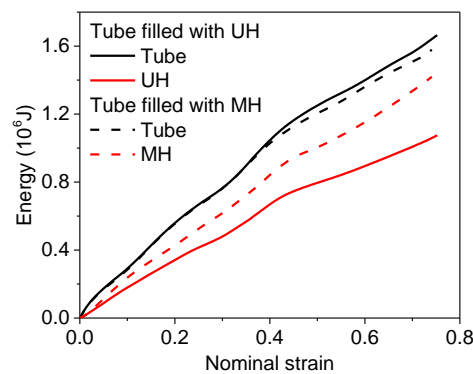


**Figure 9.** Energy absorption of tubes and honeycomb fillers.  $T_t$  is 1.5 mm,  $\bar{\rho} = 0.04$ ,  $\lambda_2$  is 0 and 0.8 for UH and MH, respectively.

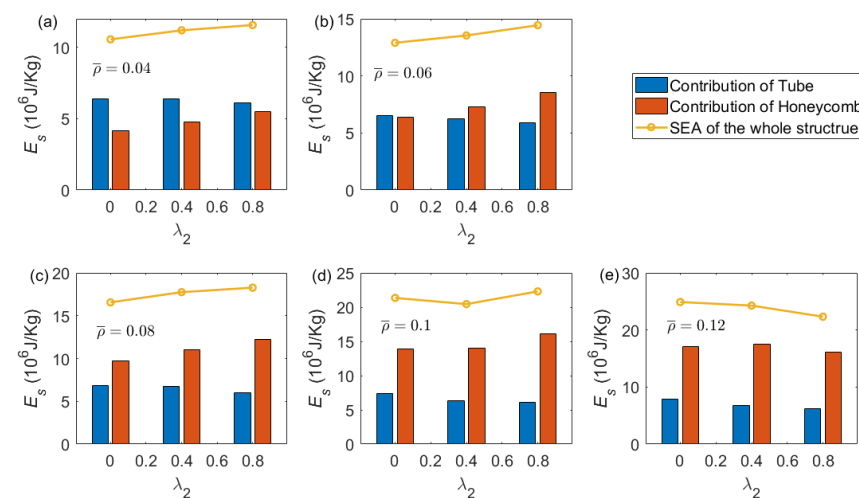


**Figure 10.** Specific energy absorption of the filled structures with different design parameters of honeycomb. (a)  $\bar{\rho} = 0.04$ , (b)  $\bar{\rho} = 0.06$ , (c)  $\bar{\rho} = 0.08$ , (d)  $\bar{\rho} = 0.1$ , (e)  $\bar{\rho} = 0.12$ .

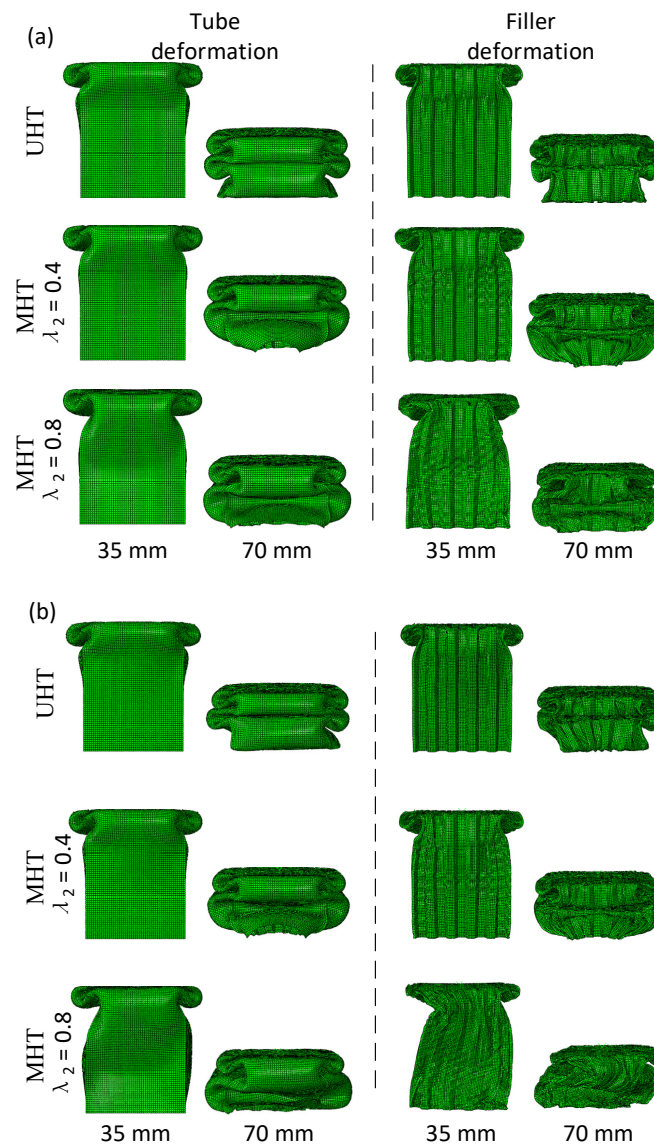


**Figure 11.** Deformation modes of tube filled with honeycomb. (a)  $T_t = 1.5$  mm,  $\bar{\rho} = 0.1$ , (b)  $T_t = 1.5$  mm,  $\bar{\rho} = 0.12$ .

When a honeycomb with  $\bar{\rho} = 0.12$  is filled into the tube, the specific energy absorption of the MHT underperforms that of the UHT, showing a decreasing trend as graded coefficient  $\lambda_2$  increases, see Figure 10e. Similar to that of  $\bar{\rho} = 0.1$ , when  $\lambda_2$  is varied from 0 to 0.4, energy absorption capacity decreases because of the weakening of the interaction, see Figure 11b. When  $\lambda_2 = 0.8$ , the deformation instability of MH is too strong to be limited by the tube, see the last row of Figure 11b. Instead of helping the filled structure absorb more energy, the unstable MH in this case is not even able to absorb as much energy as that absorbed by its corresponding UH. As a result, the specific energy absorbed by the MHT is less than that of the UHT when  $\bar{\rho} = 0.12$ .

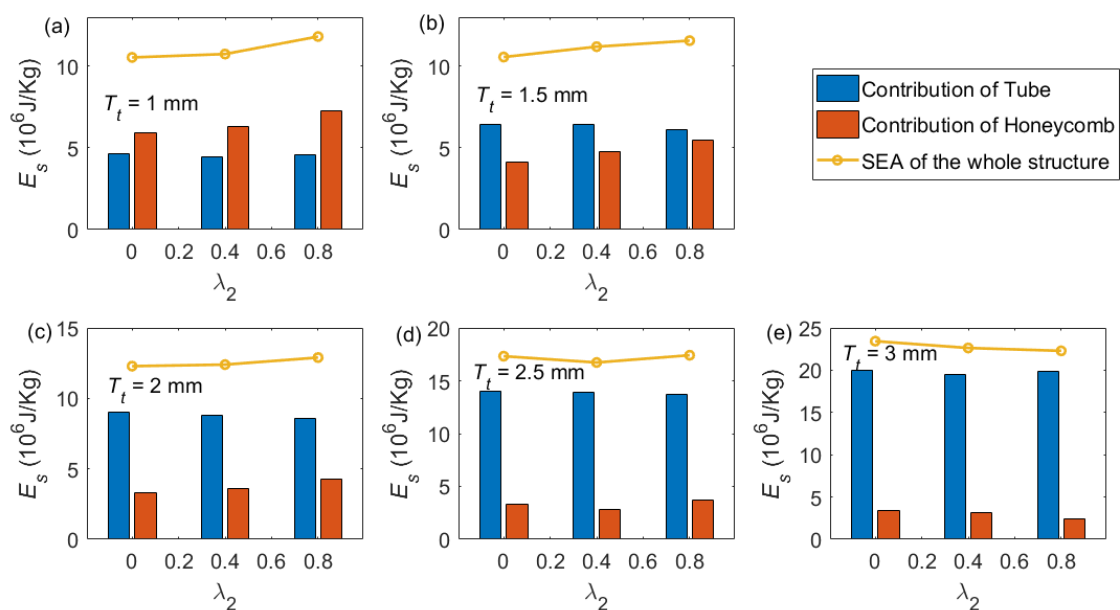
Overall, filling MH into the tube could be able to improve the energy absorption capacity of the MHT without adding weight compared with that of the corresponding UHT. When  $\bar{\rho} \leq 0.1$ , filling MH into the tube can successfully improve specific energy absorption of MHTs compared with their UHT counterparts at the end of the compression; the maximum improvement is 9.47%, 11.94%, 10.33% and 4.5% for  $\bar{\rho} = 0.04, 0.06, 0.08$  and 0.1, respectively, see Table 2. However, when the strength match between tube and honeycomb filler is inappropriate, see the last two rows of Table 2, MHTs may fail to absorb more energy than UHTs.

**Table 2.** Comparisons of specific energy absorption of the filled structure at the end of the compression under different designs of honeycombs.

$\bar{\rho}$	$\lambda_2 = 0$		$\lambda_2 = 0.4$		$\lambda_2 = 0.8$	
	$E_s$ ( $10^6$ J/Kg)	$E_s$ ( $10^6$ J/Kg)	Difference with That of $\lambda_2 = 0$ (%)	$E_s$ ( $10^6$ J/Kg)	Difference with That of $\lambda_2 = 0$ (%)	
0.04	10.56	11.19	5.97	11.56	9.47	
0.06	12.90	13.54	4.96	14.44	11.94	
0.08	16.56	17.75	7.19	18.27	10.33	
0.1	21.34	20.44	−4.22	22.30	4.50	
0.12	24.89	24.27	−2.49	22.33	−10.29	

3.3. Effects of Tube Thickness

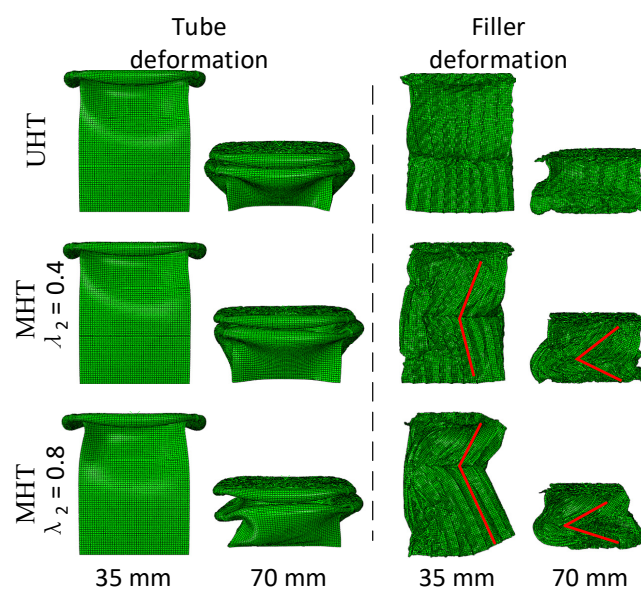
To investigate how the tube wall influences energy absorption capacity, tube wall thickness  $T_t$  is varied from 1 mm to 3 mm. The average relative density of the honeycomb is set to 0.04. Figure 12 shows the specific energy absorption of UHTs and MHTs under different tube wall thicknesses. When  $T_t \leq 2$  mm, tube walls experiences deformation mode 1 that is similar to those shown in Figure 8. The specific energy absorption of MHTs is higher than that of UHTs, and it shows a monotonic increasing trend as graded coefficient  $\lambda_2$  increases, see Figure 12a–c. However, as tube wall thickness becomes thicker, the maximum improvement of the MHT on energy absorption is 12.14%, 9.47% and 4.96% for  $T_t = 1$  mm, 1.5 mm and 2 mm, respectively, showing a decreasing trend, see Table 3. This stems from the fact that when tube wall thickness increases, the tube is making more and more contributions to energy absorption, i.e., the tube gradually dominates the energy absorption process completely, see blue bars in Figure 12. In this case, the contribution of the honeycomb filler on energy absorption decreases with the increase in tube wall thickness. When  $T_t = 2.5$  mm or 3 mm, the tube exhibits deformation mode 2, see the examples in Figure 13. Under this deformation mode, the MH filler tends to buckle during compression. Consequently, the specific energy absorption of the MHT does not outperform that of the UHT.



**Figure 12.** Specific energy absorption of the filled structure with different tube wall thicknesses. (a)  $T_t = 1$  mm, (b)  $T_t = 1.5$  mm, (c)  $T_t = 2$  mm, (d)  $T_t = 2.5$  mm, (e)  $T_t = 3$  mm.

**Table 3.** Comparisons of specific energy absorption of the filled structure under different tube wall thicknesses.

$T_t$ (mm)	$\lambda_2 = 0$		$\lambda_2 = 0.4$		$\lambda_2 = 0.8$		
	$E_s$ ( $10^6$ J/Kg)	$E_s$ ( $10^6$ J/Kg)	Difference with That of $\lambda_2 = 0$ (%)		$E_s$ ( $10^6$ J/Kg)	Difference with That of $\lambda_2 = 0$ (%)	
1	10.54	10.74	1.90		11.82	12.14	
1.5	10.56	11.19	5.97		11.56	9.47	
2	12.29	12.40	0.90		12.90	4.96	
2.5	17.33	16.73	−3.46		17.42	0.52	
3	19.72	19.05	−3.40		18.76	−4.87	

**Figure 13.** Deformation mode of tube filled with honeycomb,  $T_t = 2.5$  mm,  $\bar{\rho} = 0.04$ .

In short, to enhance the energy absorption of the filled tube, on one hand, the lateral strength of the honeycomb filler should be strong enough (i.e., a small, graded coefficient should be selected) to let the tube walls fold in a shorter length, so as to generate more lobes. On the other hand, a large, graded coefficient should be considered to allow MH to absorb more energy. Therefore, a tradeoff has to be made between them. A reasonable strength match between the MH filler and tube wall thickness should be selected to decrease the possibility of the deformation instability of the MH filler during compression.

#### 4. Conclusions

In this paper, modularized honeycomb is filled into a square tube to enhance the energy absorption capacity of the filled structure. Finite element models of the proposed structures are created and then validated by theoretical models. The specific energy absorption capacity under quasi-static compression is investigated; results and conclusions are organized as follows.

It is found that when honeycomb is compressed individually, MH with a large, graded coefficient usually experiences buckling deformation mode during compression, which dramatically weakens its energy absorption capacity. Filling MH into square tubes could remarkably improve the deformation stability of MH, and then benefit the energy absorption of MHTs. The deformation stability of MH in a square tube depends on the deformation mode of the tube. The deformation mode 1 of the tube could reduce the possibility of the deformation instability of the MH filler, but a proper strength match between tube and MH

filler should also be considered to avoid the buckling of the MH filler being too strong to be limited by the tube.

To examine the ability in energy absorption, the MHT is compared with the empty square tube and traditional uniform honeycomb-filled square tube. The results show that the modularized honeycomb-filled square tube could be able to absorb more energy per unit mass than the empty square tube and uniform honeycomb-filled square tube at the end of the compression. Through analyzing the contributions of the tube and honeycomb filler, it is found that the enhancement of the energy absorption of the MHT mainly stems from the enhancement of the modularized design to the honeycomb filler. The effects of design parameters on the energy absorption property of the MHT show that the large value of the graded coefficient for the MH filler could give rise to more excellent energy absorption capacity, and thus, help MHTs absorb more energy. However, the small, graded coefficient of the MH filler could lead to more lobes generated on tube walls, and thus help MHTs absorb more energy. Therefore, a tradeoff has to be made. Moreover, when tube walls are too thick, the deformation mode of the tube changes from deformation mode 1 to deformation mode 2. The deformation stability of MH is hard to improve under deformation mode 2, and thus, the energy absorption of the MHT cannot show its full power.

In short, we have proved that replacing uniform honeycomb by modularized honeycomb is able to improve the specific energy absorption of the honeycomb-filled square tube. This work could inspire designs of modularized filler with various types of cells and provide references for the development of energy absorbers with a lighter weight and more excellent energy absorption capacity.

**Author Contributions:** Conceptualization, Z.L.; methodology, Z.L.; software, Z.K.; validation, Z.K.; formal analysis, Z.L.; investigation, Z.L. and Z.K.; resources, Z.L.; writing—original draft preparation, Z.L.; writing—review and editing, Z.K.; supervision, X.S. All authors have read and agreed to the published version of the manuscript.

**Funding:** This research was funded by the Natural Science Foundation of Jiangsu Province, grant number BK20220344; Postdoctoral Science Foundation of China, grant number 2022M721588 and Outstanding Postdoctoral Researcher Program of Jiangsu Province, grant number 2022ZB373.

**Institutional Review Board Statement:** Not applicable.

**Informed Consent Statement:** Not applicable.

**Data Availability Statement:** The raw/processed data required to reproduce these findings cannot be shared at this time due to technical or time limitations.

**Acknowledgments:** The authors would like to acknowledge the financial support from the Natural Science Foundation of Jiangsu Province (BK20220344), Postdoctoral Science Foundation of China (2022M721588) and Outstanding Postdoctoral Researcher Program of Jiangsu Province (2022ZB373).

**Conflicts of Interest:** The authors declare no conflict of interest.

## References

1. Li, Z.; Gao, Q.; Yang, S.; Wang, L.; Tang, J. Comparative study of the in-plane uniaxial and biaxial crushing of hexagonal, re-entrant, and mixed honeycombs. *J. Sandw. Struct. Mater.* **2019**, *21*, 1991–2013. [[CrossRef](#)]
2. Luo, H.C.; Ren, X.; Zhang, Y.; Zhang X., Y.; Zhang X., G.; Luo, C.; Cheng, X.; Xie, Y. Mechanical properties of foam-filled hexagonal and re-entrant honeycombs under uniaxial compression. *Compos. Struct.* **2022**, *280*, 114922. [[CrossRef](#)]
3. Li, Z.; Wang, T.; Jiang, Y.; Wang, L.; Liu, D. Design-oriented crushing analysis of hexagonal honeycomb core under in-plane compression. *Compos. Struct.* **2018**, *187*, 429–438. [[CrossRef](#)]
4. Qi, C.; Jiang, F.; Yang, S. Advanced honeycomb designs for improving mechanical properties: A review. *Compos. Part B Eng.* **2021**, *227*, 109393. [[CrossRef](#)]
5. San Ha, N.; Lu, G. Thin-walled corrugated structures: A review of crashworthiness designs and energy absorption characteristics. *Thin-Walled Struct.* **2020**, *157*, 106995. [[CrossRef](#)]
6. Bhutada, S.; Goel, M.D. Crashworthiness parameters and their improvement using tubes as an energy absorbing structure: An overview. *Int. J. Crashworthiness* **2021**, *27*, 1569–1600. [[CrossRef](#)]

7. Wang, T.; Li, Z.; Wang, L.; Hulbert, G. Crashworthiness analysis and collaborative optimization design for a novel crash-box with re-entrant auxetic core. *Struct. Multidiscip. Optim.* **2020**, *62*, 2167–2179. [[CrossRef](#)]
8. Santosa, S.; Wierzbicki, T. Crash behavior of box columns filled with aluminum honeycomb or foam. *Comput. Struct.* **1998**, *68*, 343–367. [[CrossRef](#)]
9. Gibson, L.J.; Ashby, M.F. *Cellular Solids: Structures and Properties*, 2nd ed.; Cambridge University Press: Cambridge, UK, 1997.
10. Li, Z.; Jiang, Y.; Wang, T.; Zhuang, W.; Liu, D. In-plane crushing behaviors of piecewise linear graded honeycombs. *Compos. Struct.* **2019**, *207*, 425–437. [[CrossRef](#)]
11. Hu, L.; You, F.; Yu, T. Effect of cell-wall angle on the in-plane crushing behaviour of hexagonal honeycombs. *Mater. Des.* **2013**, *46*, 511–523. [[CrossRef](#)]
12. Hu, L.; You, F.; Yu, T. Analyses on the dynamic strength of honeycombs under the y -directional crushing. *Mater. Des.* **2014**, *53*, 293–301. [[CrossRef](#)]
13. Wang, Z.; Yao, S.; Lu, Z.; Hui, D.; Feo, L. Matching effect of honeycomb-filled thin-walled square tube—Experiment and simulation. *Compos. Struct.* **2016**, *157*, 494–505. [[CrossRef](#)]
14. Fan, T. Dynamic crushing behavior of functionally graded honeycomb structures with random defects. *Int. J. Mater. Res.* **2016**, *107*, 783–789. [[CrossRef](#)]
15. Qi, D.; Lu, Q.; He, C.W.; Li, Y.; Wu, W.; Xiao, D. Impact energy absorption of functionally graded chiral honeycomb structures. *Extrem. Mech. Lett.* **2019**, *32*, 100568. [[CrossRef](#)]
16. Shao, Y.; Meng, J.; Ma, G.; Ren, S.; Fang, L.; Cao, X.; Liu, L.; Li, H.; Wu, W.; Xiao, D. Insight into the negative Poisson's ratio effect of the gradient auxetic reentrant honeycombs. *Compos. Struct.* **2021**, *274*, 114366. [[CrossRef](#)]
17. Xiao, D.; Dong, Z.; Li, Y.; Wu, W.; Fang, D. Compression behavior of the graded metallic auxetic reentrant honeycomb: Experiment and finite element analysis. *Mater. Sci. Eng. A* **2019**, *758*, 163–171. [[CrossRef](#)]
18. Mousanezhad, D.; Ghosh, R.; Ajdari, A.; Hamouda, A.; Nayeb-Hashemi, H.; Vaziri, A. Impact resistance and energy absorption of regular and functionally graded hexagonal honeycombs with cell wall material strain hardening. *Int. J. Mech. Sci.* **2014**, *89*, 413–422. [[CrossRef](#)]
19. Tao, Y.; Duan, S.; Wen, W.; Pei, Y.; Fang, D. Enhanced out-of-plane crushing strength and energy absorption of in-plane graded honeycombs. *Compos. Part B Eng.* **2017**, *118*, 33–40. [[CrossRef](#)]
20. Duan, S.; Tao, Y.; Lei, H.; Wen, W.; Liang, J.; Fang, D. Enhanced out-of-plane compressive strength and energy absorption of 3D printed square and hexagonal honeycombs with variable-thickness cell edges. *Extrem. Mech. Lett.* **2018**, *18*, 9–18. [[CrossRef](#)]
21. Li, Z.; Liu, D.; Qian, Y.; Wang, Y.; Wang, T.; Wang, L. Enhanced strength and weakened dynamic sensitivity of honeycombs by parallel design. *Int. J. Mech. Sci.* **2019**, *151*, 672–683. [[CrossRef](#)]
22. Wu, Y.; Sun, L.; Yang, P.; Fang, J.; Li, W. Energy absorption of additively manufactured functionally bi-graded thickness honeycombs subjected to axial loads. *Thin-Walled Struct.* **2021**, *164*, 107810. [[CrossRef](#)]
23. Li, Z.; Sun, H.; Wang, T.; Wang, L.; Su, X. Modularizing honeycombs for enhancement of strength and energy absorption. *Compos. Struct.* **2022**, *279*, 114744. [[CrossRef](#)]
24. Reid, S.R.; Reddy, T.Y.; Gray, M.D. Static and dynamic axial crushing of foam-filled sheet metal tubes. *Int. J. Mech. Sci.* **1986**, *28*, 295–322. [[CrossRef](#)]
25. Zarei, H.R.; Kröger, M. Crashworthiness optimization of empty and filled aluminum crash boxes. *Int. J. Crashworthiness* **2007**, *12*, 255–264. [[CrossRef](#)]
26. Hussein, R.D.; Ruan, D.; Lu, G.; Guillow, S.; Yoon, J. Crushing response of square aluminium tubes filled with polyurethane foam and aluminium honeycomb. *Thin-Walled Struct.* **2017**, *110*, 140–154. [[CrossRef](#)]
27. Wang, Z.; Liu, J.; Lu, Z.; Hu, D. Mechanical behavior of composited structure filled with tandem honeycombs. *Compos. Part B Eng.* **2017**, *114*, 128–138. [[CrossRef](#)]
28. Simpson, J.; Kazanci, Z. Crushing investigation of crash boxes filled with honeycomb and re-entrant (auxetic) lattices. *Thin-Walled Struct.* **2020**, *150*, 106676. [[CrossRef](#)]
29. Gao, Q.; Liao, W.H.; Wang, L.; Huang, C. Crashworthiness optimization of cylindrical negative Poisson's ratio structures with inner liner tubes. *Struct. Multidiscip. Optim.* **2021**, *64*, 4271–4286. [[CrossRef](#)]
30. Wang, C.Y.; Li, Y.; Zhao, W.Z.; Zou, S.; Zhou, G.; Wang, Y. Structure design and multi-objective optimization of a novel crash box based on biomimetic structure. *Int. J. Mech. Sci.* **2018**, *138*, 489–501. [[CrossRef](#)]
31. Tsang, H.H.; Raza, S. Impact energy absorption of bio-inspired tubular sections with structural hierarchy. *Compos. Struct.* **2018**, *195*, 199–210. [[CrossRef](#)]
32. Li, Z.; Duan, L.; Chen, T.; Hu, Z. Crashworthiness analysis and multi-objective design optimization of a novel lotus root filled tube (LFT). *Struct. Multidiscip. Optim.* **2018**, *57*, 865–875. [[CrossRef](#)]
33. Nian, Y.; Wan, S.; Li, X.; Su, Q.; Li, M. How does bio-inspired graded honeycomb filler affect energy absorption characteristics? *Thin-Walled Struct.* **2019**, *144*, 106269. [[CrossRef](#)]
34. Gao, Q.; Liao, W.H.; Huang, C. Theoretical predictions of dynamic responses of cylindrical sandwich filled with auxetic structures under impact loading. *Aerosp. Sci. Technol.* **2020**, *107*, 106270. [[CrossRef](#)]
35. Zhang, Y.; Ge, P.; Lu, M.; Lai, X. Crashworthiness study for multi-cell composite filling structures. *Int. J. Crashworthiness* **2018**, *23*, 32–46. [[CrossRef](#)]



36. Yin, H.; Wen, G.; Hou, S.; Chen, K. Crushing analysis and multiobjective crashworthiness optimization of honeycomb-filled single and bitubular polygonal tubes. *Mater. Des.* **2011**, *32*, 4449–4460. [[CrossRef](#)]
37. Zhang, Y.; Xu, X.; Lu, M.; Hu, Z.; Ge, P. Enhance crashworthiness of composite structures using gradient honeycomb material. *Int. J. Crashworthiness* **2018**, *23*, 569–580. [[CrossRef](#)]
38. Yao, S.; Xiao, X.; Xu, P.; Qu, Q.; Che, Q. The impact performance of honeycomb-filled structures under eccentric loading for subway vehicles. *Thin-Walled Struct.* **2018**, *123*, 360–370. [[CrossRef](#)]
39. Gao, Q.; Liao, W.H. Energy absorption of thin walled tube filled with gradient auxetic structures-theory and simulation. *Int. J. Mech. Sci.* **2021**, *201*, 106475. [[CrossRef](#)]
40. Xie, S.; Du, X.; Zhou, H.; Wang, J.; Chen, P. Crashworthiness of Nomex<sup>®</sup> honeycomb-filled anti-climbing energy absorbing devices. *Int. J. Crashworthiness* **2021**, *26*, 121–132. [[CrossRef](#)]
41. Wang, D.; Xu, P.; Yang, C.; Xiao, X.; Che, Q. Crashing performance and multi-objective optimization of honeycomb-filled thin-walled energy absorber with axisymmetric thickness. *Mech. Adv. Mater. Struct.* **2022**, 1–18. [[CrossRef](#)]
42. Zhou, G.; Yan, P.; Wang, Q.; Dai, S.; Li, X.; Hao, Y.; Wang, Y. Optimal design of a novel crash box with functional gradient negative Poisson's ratio structure. *Proc. Inst. Mech. Eng. Part D J. Automob. Eng.* **2022**, *236*, 3309–3325. [[CrossRef](#)]
43. Zhu, G.; Li, S.; Sun, G.; Li, G.; Li, Q. On design of graded honeycomb filler and tubal wall thickness for multiple load cases. *Thin-Walled Struct.* **2016**, *109*, 377–389. [[CrossRef](#)]
44. Fang, J.; Gao, Y.; An, X.; Sun, G.; Chen, J.; Li, Q. Design of transversely-graded foam and wall thickness structures for crashworthiness criteria. *Compos. Part B Eng.* **2016**, *92*, 338–349. [[CrossRef](#)]
45. Yin, H.; Dai, J.; Wen, G.; Tian, W.; Wu, Q. Multi-objective optimization design of functionally graded foam-filled graded-thickness tube under lateral impact. *Int. J. Comput. Methods* **2019**, *16*, 1850088. [[CrossRef](#)]
46. Xiao, Y.; Zang, M.; Li, Z. Effects of aluminum honeycomb filler on crashworthiness of CFRP thin-walled beams under dynamic impact. *Int. J. Crashworthiness* **2021**, *27*, 985–994. [[CrossRef](#)]
47. Chen, Y.; Ye, L.; Fu, K. Progressive failure of CFRP tubes reinforced with composite sandwich panels: Numerical analysis and energy absorption. *Compos. Struct.* **2021**, *263*, 113674. [[CrossRef](#)]
48. Ma, J.; You, Z. Energy absorption of thin-walled beams with a pre-folded origami pattern. *Thin-Walled Struct.* **2013**, *73*, 198–206. [[CrossRef](#)]
49. Hanssen, A.G.; Langseth, M.; Hopperstad, O.S. Static and dynamic crushing of circular aluminium extrusions with aluminium foam filler. *Int. J. Impact Eng.* **2000**, *24*, 475–507. [[CrossRef](#)]
50. Wierzbicki, T. Crushing analysis of metal honeycombs. *Int. J. Impact Eng.* **1983**, *1*, 157–174. [[CrossRef](#)]

**Disclaimer/Publisher's Note:** The statements, opinions and data contained in all publications are solely those of the individual author(s) and contributor(s) and not of MDPI and/or the editor(s). MDPI and/or the editor(s) disclaim responsibility for any injury to people or property resulting from any ideas, methods, instructions or products referred to in the content.